Phase Transition upon K^+ Ion Exchange into Na-Low Silica X: Combined NMR and Synchrotron X-ray Powder Diffraction Study

Yongjae Lee,[†] Stuart W. Carr,[‡] and John B. Parise*[,§]

Geosciences and Chemistry Departments, State University of New York, Stony Brook, New York 11794, and ANSTO, Private Mail Bag 1, Menai 2234, Australia

Received May 13, 1998. Revised Manuscript Received June 26, 1998

The mechanism by which K^+ ions exchange into zeolite Na-low silica X (LSX) ($Na_{96}Al_{96}Si_{96}O_{384}\cdot nH_2O$) has been determined by studying structures of the Na-LSX and K-LSX end members in the Na−K LSX solid solution series as well as samples exchanged at the 20%, 42% and 80% K^+ levels. A preliminary investigation using ^{29}Si MAS NMR spectroscopy revealed a two-phase region in the solid solution near 80% K^+ exchange. Rietveld analysis of the powder diffraction data collected from hydrated samples showed that, up to 42% of K^+ exchange, K^+ ions were located preferentially at site I′, just outside the double 6-ring (D6R) in the sodalite cage, and at site II, above the single 6-ring (S6R) in the supercage. Introduction of K^+ ions into site I′ repositioned Na^+ ions into site I, at the center of the D6R. An abrupt change in the cubic lattice parameter from 25.0389(5) to 25.2086(5) Å marked the formation of a second phase at the 80% K^+-exchange level as K^+ ions began to occupy site I. No coexistence of phases was observed for the fully K^+-exchanged sample (a = 25.2486(2) Å), where sites I and II were fully occupied by K^+ ions.

Introduction

Zeolites are crystalline microporous aluminosilicates and are of considerable technological interest due to their properties of ion exchange, adsorption, molecular sieving, and catalysis.[1] Ion exchange is a major industrial application, and modification in the catalytic or molecular sieving properties of the parent zeolite can be accomplished with a variety of exchangeable cations.[2] The faujasite framework (Figure 1) is particularly versatile in this respect and has been prepared with Si/Al ratios ranging from 1.0 to 1.5 for zeolite X and from greater than 1.5 to about 3 for zeolite Y. Low silica *X* (LSX) has a Si/Al ratio of unity, and hence the maximum possible number of exchangeable cations. An extensive study of the phase diagram for the formation of LSX[3] showed that the synthesis of this material has a strong dependency on the Na/K ratio. By varying the Na/K ratio, it was possible to directly prepare mixtures of LSX and A type zeolites. This work has also suggested that potassium plays a key role in directing the structural formation of LSX. Other researchers have examined this material for its improved air separation capacities[4] and for use as an enhanced water-softening agent.[5]

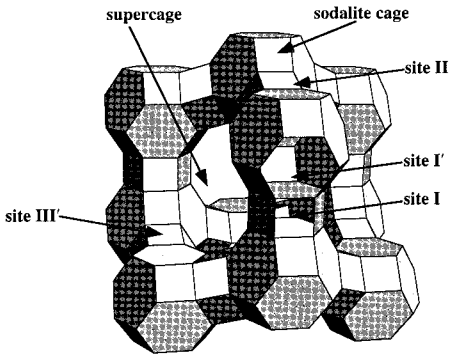

Figure 1. Polyhedral representation of the faujasite framework. Nodes represent the centers of Si/Al tetrahedra and straight line sections represent the T−O−T linkages (T = Si/Al). Cation sites are located in the middle of the double 6-ring (site I), close to the 6-rings both in the sodalite cage (site I′) and in the supercage (site II), and close to the 4-rings (site III′). Designation of each atomic position in this study follows Olson's nomenclature (see Tables 1−3).[18]

Faujasite consists of a negatively charged aluminosilicate framework (Figure 1) with two interconnecting, three-dimensional networks of cavities,[6] containing charge compensating cations. The larger cavities, called the supercages or 26-hedron cages, have a free diameter of about 13 Å and are linked by sharing rings of 12 tetrahedra (12-ring windows) that have a free diameter of about 8 Å. The smaller sodalite cavities, called β-cages or truncated octahedron cages, have a free diameter of about 7 Å and are linked in a diamond-lattice type through rings of six tetrahedra (6-ring

[†] Geosciences Department, SUNY.
[‡] ANSTO.
[§] Chemistry Department, SUNY.

(1) Bouchet, F.; Fujisawa, H.; Kato, M.; Yamaguchi, T. *Stud. Surf. Sci. Catal.* **1994**, *84*, 2029.
(2) Barrer, R. M. *Hydrothermal Chemistry of Zeolites*; Academic Press: London, 1982.
(3) Carr, S. W.; Hollway, F.; Hopwood, J. D. Unpublished data.
(4) Coe, C. G.; Kuznicki, S. M.; Srinivasan, R.; Jenkins, R. J. *ACS Symp. Ser.* **1988**, *368*, 478.
(5) Butter, S. A.; Kunzicki, S. M. European Patent Application 86104118.4, 1986
(6) Breck, D. W. *Zeolite Molecular Sieves*; Krieger: Malabar, FL, 1984.

S0897-4756(98)00342-1 CCC: $15.00
Published on Web 08/20/1998

windows) to form the hexagonal double 6-ring prisms (D6R) between the sodalite cages. The 6-ring windows of the sodalite cages have a free diameter of about 2.5 Å and are therefore capable of selecting for certain exchangeable cations or molecules into the sodalite cages and into the hexagonal prisms. In these structures the cations are located at preferred extraframwork sites, which in the case of X type zeolites are the so-called type I, I′, II, and III′ sites (Figure 1).

As part of our on-going studies of the time-resolved structural responses of microporous materials to ion exchange[7] and sorption,[8] we have been performing ex situ studies to provide the foundation for the structure refinements using the time-resolved data. We report here the results of ^{29}Si MAS NMR and synchrotron X-ray powder diffraction studies of K^+ exchange in Na-LSX zeolite at various levels.

Experimental Section

Initial Sample Preparation. Zeolite LSX was prepared in the following manner. To a rapidly stirred solution prepared from NaOH (44.8 g), KOH (26.4 g), water (127.1 g), and aqueous sodium aluminate (80.0 g, 20% Al_2O_3, 20% Na_2O) cooled to room temperature was added an aqueous solution of sodium silicate (62.8 g, 30% SiO_2, 12% Na_2O) and water (127.5 g). After several minutes the initially clear solution gave an opaque mixture. This was stirred for approximately 15 min and then crystallized in a sealed vessel at 85 °C for 22 h. The resultant zeolite was collected by filtration and washed three times with 200 g of distilled water adjusted to pH 9 with NaOH. The zeolite was dried at 85 °C for 16 h in air and equilibrated over saturated ammomium nitrate. It was initially characterized using X-ray powder diffraction and shown to be highly crystalline LSX with a unit cell size of 25.03 Å. The scanning electron mircograph indicated that LSX consisted of approximately uniform 3 μm sized multifaceted spherical particulates. The unit cell composition was determined to be $Na_{74}K_{22}Al_{96}Si_{96}O_{384}$, anhydrous with a water content of 25% by ICP elemental analysis, and denoted NaK-LSX. Characterization using ^{29}Si and ^{27}Al MAS NMR spectroscopy on this starting material was consistent with a Si/Al ratio of 1, showing strict alternation of Si and Al in the available framework sites.

Qualitative Ion Exchange Experiment for NMR Samples. A series of LSX samples for NMR spectroscopy was prepared to investigate the solubility region of the Na−K LSX solid solution series. The end members of the Na−K LSX series were prepared by ion exchange using a 5 g sample of the as prepared NaK-LSX. Solutions used were 500 mL of a 1 M NaCl solution adjusted to pH 9 with NaOH and 500 mL of a 1 M KCl solution adjusted to pH 9 with KOH to avoid hydrolysis. Three ion exchange procedures over 2 h at 60 °C completely removed all residual potassium and sodium, as determined from atomic adsorption analysis and gave samples we denoted as Na- and K-LSX, respectively. Partially K^+-exchanged samples were prepared by varying the amount and concentration of KCl solution in a way to give different K^+-exchange levels along the Na−K LSX series. Lower K^+-exchanged LSX was prepared by stirring a 1.5 g sample of the as-prepared NaK-LSX in 100 mL of a 0.5 M KCl solution adjusted to pH 9 with KOH over 2 h at 60 °C. Medium K^+-exchanged LSX was prepared by stirring a 5 g sample of the as-prepared NaK-LSX in 200 mL of a 1.0 M KCl solution adjusted to pH 9 with KOH over 2 h at 60 °C. Higher K^+-exchanged LSX was prepared by stirring a 2.5 g sample of the above product in 100 mL of a 1.0 M KCl solution adjusted to pH 9 with KOH over 2 h at 60 °C. Each resultant zeolite was collected, washed with distilled water, and dried in air. These samples were designated NaK-LSX-L, NaK-LSX-M, and NaK-LSX-H, respectively.

Quantitative Ion Exchange Experiment for X-ray Samples. Samples which represented several points along the Na−K LSX solid solution series were prepared for structure analysis. The pure sodium form of LSX was prepared in the following manner. A 5 g sample of the as-prepared NaK-LSX was stirred at 70 °C over 24 h in 500 mL of a 1.0 M NaCl solution adjusted to pH 9 with NaOH to avoid hydrolysis. This was repeated three times followed by subsequent washing with distilled water. An ICP chemical analysis showed that the exchange was complete. This material, denoted Na-LSX ($Na_{96}Al_{96}Si_{96}O_{384}\cdot nH_2O$), was then used to make three partially K^+-exchanged LSX samples, following the ion exchange isotherm by Sherry.[9] Each 0.1 g sample of Na-LSX was stirred at 25 °C over 24 h in 500 mL of a 0.1 total normality NaCl and KCl exchange solution. The potassium fractions in the solutions used were 0.10, 0.55, and 0.90, and each solution was adjusted to pH 9 with NaOH. This was repeated twice to ensure that equilibrium was achieved at each desired exchange level. The resultant zeolite was collected, washed with distilled water, and dried in air. Direct current plasma and ICP chemical analysis for potassium and sodium showed 20%, 42%, and 80% K^+-exchange levels for the three samples. A fully K^+-exchanged sample was also prepared using a 5 g sample of the as-prepared NaK-LSX. Five rounds of K^+ exchange at 70 °C over 24 h in 500 mL of a 1.0 M KCl solution adjusted to pH 9 with KOH removed all sodium, as determined from ICP chemical analysis, and gave the pure potassium form of LSX. These samples were denoted NaK-LSX20, NaK-LSX42, NaK-LSX80, and K-LSX, respectively, according to their potassium percentages. Each hydrated, ion-exchanged sample was equilibrated at ambient temperature to provide a comparison with the time-resolved experiment of K^+ exchange into Na-LSX.[7]

Solid-State NMR Measurements. The solid-state MAS NMR spectra were recorded on a Bruker MSL 400 spectrometer. The ^{29}Si spectra were collected at 79.494 MHz with a pulse width of 4 μs, delay of 2 s, and spinning speed of 4000 Hz and referenced to TMS. The ^{27}Al spectra were collected at 104.26 MHz with a pulse width of 0.06 μs, delay of 0.1 s, and spinning speed of 8000 Hz and referenced to hydrated acidic $Al(NO_3)_3$.

Synchrotron X-ray Powder Diffraction Measurements. Synchrotron X-ray powder diffraction data were collected at beamline X7A of the National Synchrotron Light Source (NSLS). Powders were loaded into 0.3 mm diameter glass capillaries and sealed with a torch under ambient conditions. A monochromatic beam was obtained using a channel-cut Si (111) monochromator, and the wavelength of 0.8013(1) Å was calibrated using a CeO_2 standard material (a = 5.4113(1) Å). A linear position sensitive detector (PSD)[10−12] collected data at room temperature by step scanning over the angular range $4° \le 2\theta \le 50°$ in increments of 0.25°. Counting times of 5, 10, 20, and 40 s were used for the frames of 1−46, 47−92, 93−138, and 139−184, respectively, in consideration of lesser intensity at higher angles. The capillaries were rotated at an angular velocity of 1−2 Hz during data collection in order to obtain better powder averaging. The central 3° portion of the linear PSD frame at each step was combined to produce a pattern with 0.01° resolution. No absorption correction was carried out.

Results and Discussion

Solid State NMR Spectroscopy. The as prepared NaK-LSX had a single ^{29}Si MAS NMR band at −84.5 ppm, typical of an ordered X type zeolite with a Si/Al

(7) Lee, Y.; Cahill, C. L.; Hanson, J. C.; Parise, J. B.; Carr, S. W.; Myrick, M. L.; Preckwinkel, U. V.; Phillips, J. C. Accepted to 12th International Zeolite Conference, Baltimore, MD, 1998.

(8) Lee, Y.; Savitz, S. A.; Parise, J. B. Manuscript in preparation.

(9) Sherry, H. S. *J. Phys. Chem.* **1966**, *70*, 1158.

(10) Smith, G. C. *Synth. Rad. News* **1991**, *4*, 24.

(11) Cox, D. E.; Toby, B. H.; Eddy, M. M. *Aust. J. Phys.* **1988**, *41*, 117.

(12) Cox, D. E. In *Synchrotron Radiation Crystallography*, Coppens, P., Ed.; Academic Press: London, 1992.

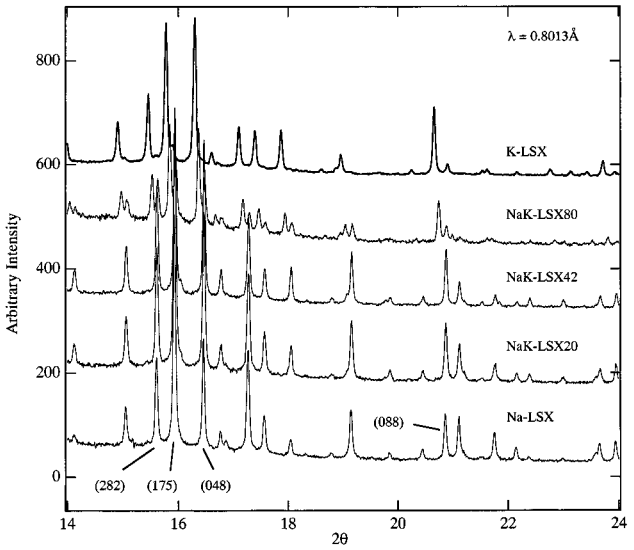

Figure 2. Five synchrotron X-ray powder diffraction patterns showing the changes in the relative intensities and peak positions as the K^+-exchange percentage increases in Na-LSX (from bottom), NaK-LSX20, NaK-LSX42, NaK-LSX80, and K-LSX. Note the two phases in NaK-LSX80.

ratio of unity and a strict alternation of silicon and aluminum on the framework sites.[13] The ^{27}Al MAS NMR spectra showed a single narrow band at −58 ppm, consistent with tetrahedral framework aluminum. Sodium-exchanged LSX (Na-LSX) also gave single ^{29}Si and ^{27}Al resonances with the same chemical shifts as were observed in the as-prepared NaK-LSX. Potassium-exchanged LSX (K-LSX) gave a single ^{29}Si resonance at −87.2 ppm. One of the partially K^+-exchanged samples, NaK-LSX-L, had a single ^{29}Si resonance at −84.5 ppm which was similar to that of Na-LSX. The presence of a region of limited solubility in the Na−K LSX solid solution series was detected with the NaK-LSX-M sample. Two ^{29}Si resonances, one at −84.7 ppm with the second at −87.2 ppm, indicated the presence of two phases in this sample. This observation was confirmed by X-ray powder diffraction (see below). The other sample, NaK-LSX-H, gave a single ^{29}Si resonance at −87.4 ppm which was similar to that of K-LSX.

Synchrotron X-ray Powder Diffraction. Preliminary examination of the diffraction patterns (Figure 2) showed that the relative intensities of different peaks changed as the K^+-exchange level increased up to 42%. The positions of the peaks, however, did not change drastically. For the sample with 80% K^+ exchange, NaK-LSX80, two sets of peaks, which could be indexed as two separate face-centered cubic phases, appeared. The new set of peaks were shifted to a lower 2θ value relative to Na-LSX, indicating a larger unit cell. Only one phase with this expanded unit cell remained in the fully K^+-exchanged sample, K-LSX. This behavior is consistent with that observed in the NMR studies discussed above.

The Rietveld method[14] and the GSAS suite of programs[15] were used to derive and refine structural models for all the potassium-exchanged LSX samples, as well as for the pure Na-LSX. A total of 852, 847, 847, 1297, and 692 Bragg reflections, starting with the first (111) peak, were included in the refinements of Na-LSX, NaK-LSX20, NaK-LSX42, NaK-LSX80, and K-LSX, respectively. The refinement for NaK-LSX80 included two phases (Table 1). The histogram scale, lattice constant, and zero point shift were refined initially, and the phase fraction was also refined for the NaK-LSX80 sample. The diffraction peaks were modeled with a pseudo-Voigt profile function,[16] using Gaussian *U*, *V*, and *W* coefficients,[17] a Lorentzian particle size broadening term, and one asymmetry correction term. The background curves of all the diffraction patterns were fitted with a shifted Chebyschev polynomial function with a variable number of coefficients (20 for Na-LSX, NaK-LSX20, and NaK-LSX42; 16 for NaK-LSX80; and 24 for K-LSX).

Olson's model of hydrated $Na_{88}X$[18] was used as a starting point for the refinement of Na-LSX. Initial refinement in space group $Fd\bar{3}$ indicated two distinct T−O distances for the framework tetrahedral sites, suggesting strict Si/Al ordering for this LSX material, as indicated by the preliminary NMR result. Soft constraints[15] were applied to maintain the Si and Al tetrahedral geometry throughout the refinement process. Difference Fourier maps were calculated, and residual electron densities attributable to extraframework species were located. The final refined model of Na-LSX was then used as a starting model for NaK-LSX20. A similar mode was applied to the refinements of the structural models for the higher K^+-exchanged samples.

The distinction between extraframework Na^+ and K^+ ions might be expected to be made on the basis of the difference between Na−O and K−O coordination distances. In the hydrated samples, however, the determination of the cation distribution can be hindered by the ambiguity introduced by the coincidence between the mean K−O distance and the hydrogen bond length between water molecules and framework oxygens. An important factor in resolving this ambiguity was sought in the well-known effect of Al content on ion siting in hydrated faujasite type zeolites.[18−20] According to this rule, cation siting is energetically favored when there are three Al ions per 6-ring (Al_3 6-ring, site II in Figure 1) or six Al ions per double 6-ring (Al_6 prism, sites I and I′ in Figure 1). Since silicon and aluminum alternate throughout the tetrahedral sites, LSX is expected to have a full occupancy of 32 cations at site II and $n(\mathrm{I}) + n(\mathrm{I}')$ cations at both sites I and I′, where $n(\mathrm{I}) = {}^1/_2[32 - n(\mathrm{I}')]$. Simultaneous occupancy by the same kinds of cations at sites I and I′ is unlikely due to the intercationic repulsion between cations occupying these sites (Figure 1). For example, the Na1−Na2 and K1−K2 distances in these sites would be 2.6 and 3.3 Å, respectively. Designation of each atomic position in this

(13) Klinowski, J. *Progress in NMR Spectroscopy* **1984**, *16*, 237.
(14) Young, R. A. *The Reitveld Method*; Young, R. A., Ed.; Oxford University Press Inc.: New York, 1995.
(15) Larson, A. C.; VonDreele, R. B. GSAS; *General Structure Analysis System*; Report LAUR 86-748; Los Alamos National Laboratory, 1986.
(16) Howard, C. J. *J. Appl. Crystallogr.* **1982**, *15*, 615.
(17) Thompson, P.; Cox, D. E.; Hastings, J. B. *J. Appl. Crystallogr.* **1987**, *20*, 79.
(18) Olson, D. H. *J. Phys. Chem.* **1970**, *74*, 2758.
(19) Olson, D. H.; Kokotailo, G. T.; Charnell, J. F. *J. Colloid Interface Sci.* **1968**, *28*, 305.
(20) Smith, J. V.; Bennett, J. M. American Crystallographic Association Meeting, Buffalo, NY, 1968, AN LL5.

Table 1. Selected Refinement Information and Refined Atomic Parameters of Each Powder Sample

		Na-LSX	NaK-LSX20	NaK-LSX42	NaK-LSX80(Na)	NaK-LSX80(K)	K-LSX
cation content/unit cell		Na_{96}	$Na_{77}K_{19}$	$Na_{56}K_{40}$	$Na_{19}K_{77}$		NaK_{95}
lattice parameter (Å)		25.0491(3)	25.0352(3)	25.0285(2)	25.0389(5)	25.2086(5)	25.2486(3)
R^a		0.0592	0.0558	0.0613	0.0855		0.0631
reduced $^b\chi^2$		3.020	3.010	3.450	2.441		3.950
T(1)	x	−0.05223(13)	−0.05254(12)	−0.05289(12)	−0.05198(21)	−0.05343(18)	−0.05430(14)
96 (g)	y	0.12456(16)	0.12443(16)	0.12466(16)	0.12526(25)	0.12437(22)	0.12455(18)
	z	0.03443(14)	0.03401(14)	0.03402(14)	0.03597(20)	0.03548(19)	0.03360(15)
	U_{iso} (Å^2)	0.0127(3)^c	0.0121(3)^c	0.0122(3)^c	0.0070(14)^c	0.0130(9)^c	0.0102(4)
T(2)	x	−0.05411(13)	−0.05383(13)	−0.05337(13)	−0.05376(19)	−0.05480(18)	−0.05506(14)
96 (g)	y	0.03738(13)	0.03752(12)	0.03765(12)	0.03842(16)	0.03727(16)	0.03763(14)
	z	0.12331(16)	0.12275(16)	0.12290(16)	0.12904(21)	0.12792(20)	0.12505(17)
O(1)	x	−0.1094(2)	−0.1096(2)	−0.1093(2)	−0.1040(4)	−0.1071(3)	−0.1098(2)
96 (g)	y	0.0007(3)	0.0005(3)	0.0011(3)	0.0001(3)	−0.0003(3)	0.0001(3)
	z	0.1044(2)	0.1053(2)	0.1051(2)	0.1012(4)	0.1044(4)	0.1071(3)
	U_{iso} (Å^2)	0.0234(6)^d	0.0229(6)^d	0.0233(6)^d	0.0261(28)^d	0.0295(15)^d	0.0210(7)^d
O(2)	x	−0.0027(2)	−0.0027(2)	−0.0022(2)	−0.0010(3)	−0.0025(3)	−0.0035(2)
96 (g)	y	−0.0033(2)	−0.0032(2)	−0.0032(2)	−0.0029(3)	−0.0048(3)	−0.0047(2)
	z	0.1450(2)	0.1449(2)	0.1448(2)	0.1456(3)	0.1423(3)	0.1408(2)
O(3)	x	−0.0326(2)	−0.0333(2)	−0.0330(2)	−0.0325(3)	−0.0355(3)	−0.0361(2)
96 (g)	y	0.0729(2)	0.0717(2)	0.0726(2)	0.0811(4)	0.0782(3)	0.0758(2)
	z	0.0681(2)	0.0663(2)	0.0669(2)	0.0790(4)	0.0764(4)	0.0713(2)
O(4)	x	−0.0720(2)	−0.0716(2)	−0.0718(2)	−0.0768(4)	−0.0737(3)	−0.0696(2)
96 (g)	y	0.0783(2)	0.0792(2)	0.0789(2)	0.0729(3)	0.0732(3)	0.0739(2)
	z	0.1759(2)	0.1750(2)	0.1751(2)	0.1843(4)	0.1833(3)	0.1813(2)
Na1	$x = y = z$	0.0	0.0	0.0	0.0		
16 (c)	occupancy	11.3(3)	14.9(3)	15.3(3)	10.9(5)		
	U_{iso} (Å^2)	0.023(4)	0.024(3)^g	0.031(3)^h	0.031(6)^j		
K1	$x = y = z$				0.0	0.0	0.0
16 (c)	occupancy				2.3(1)	11.4(3)	15.5(2)
	U_{iso} (Å^2)				0.031(6)^j	0.028(3)^k	0.030(1)^l
Na2	$x = y = z$	0.0612(3)	0.0602(3)	0.0612(3)	0.0546(3)		
32 (e)	occupancy	9.3(5)	2.2(5)	1.4(5)	5.8(13)		
	U_{iso} (Å^2)	0.034(3)^e	0.024(3)^g	0.031(3)^h	0.031(6)^j		
K2	$x = y = z$		0.0736(3)	0.0738(3)	0.0767(4)	0.0729(4)	
32 (e)	occupancy		8.2(4)	9.4(5)	9.3(9)	9.2(5)	
	U_{iso} (Å^2)		0.023(6)	0.027(5)	0.031(6)^j	0.028(3)^k	
Na3B	$x = y = z$	0.2354(2)	0.2353(4)	0.2352(4)	0.2244(23)	0.2303(28)	
32 (e)	occupancy	29.6(6)	21.9(9)	11.5(8)	7.7(9)	4.8(11)	
	U_{iso} (Å^2)	0.034(3)^e	0.041(5)	0.017(7)	0.031(6)^j	0.028(3)^k	
K3B	$x = y = z$		0.2555(4)	0.2561(2)	0.2547(5)	0.2524(4)	0.2514(1)
32 (e)	occupancy		9.0(6)	17.3(5)	24.3(9)	25.6(8)	31.0(2)
	U_{iso} (Å^2)		0.016(6)	0.023(3)	0.031(6)^j	0.028(3)^k	0.030(1)^l
OW(1)	$x = y = z$	0.072(1)					0.0748(4)
32 (e)	occupancy	14.0(10)					23.4(7)
OW(2)	x	0.096(1)	0.095(1)	0.093(1)	0.110(1)	0.088(1)	0.090(1)
96 (g)	y	0.093(1)	0.093(1)	0.091(1)	0.104(1)	0.089(1)	0.090(1)
	z	0.172(1)	0.180(1)	0.180(1)	0.180(1)	0.181(1)	0.180(1)
	occupancy	25.9(7)	35.1(8)	37.4(8)	27.4(23)	41.8(16)	48.3(8)
	U_{iso} (Å^2)	0.141(5)^f	0.190(7)^f	0.179(7)^f	0.081(9)^f	0.090(8)^f	0.096(4)^f
OW(4)	x	0.273(3)	0.275(5)	0.269(4)	0.204(3)	0.192(2)	0.187(2)
96 (g)	y	0.304(2)	0.302(4)	0.302(9)	0.329(4)	0.322(2)	0.332(2)
	z	0.283(3)	0.284(7)	0.296(10)	0.317(4)	0.337(2)	0.341(2)
	occupancy	37.1(13)	21.9(9)	14.7(5)	67.2(77)	73.0(58)	49.9(48)
OW(4B)	$x = y = z$		0.320(1)	0.320(1)	0.315(2)	0.311(1)	0.314(1)
32 (e)	occupancy		9.6(13)	15.7(13)	24.3(9)	26.9(20)	10.2(8)
OW(5)	x	0.342(2)	0.342(2)	0.344(2)	0.352(3)	0.373(4)	0.344(2)
96 (g)	y	0.338(2)	0.335(2)	0.333(2)	0.357(3)	0.328(3)	0.316(2)
	z	0.192(1)	0.193(1)	0.193(1)	0.185(2)	0.200(3)	0.214(3)
	occupancy	62.7(22)	91.6(21)	91.3(21)	85.4(48)	38.4(5)	37.4(39)
OW(6)	x	0.266(2)	0.272(4)	0.284(3)	0.234(4)	0.288(4)	0.265(4)
96 (g)	y	0.248(2)	0.265(5)	0.264(3)	0.268(4)	0.278(4)	0.265(4)
	z	0.400(1)	0.408(2)	0.412(2)	0.368(4)	0.399(3)	0.390(2)
	occupancy	49.2(23)	33.3(28)	34.7(24)	42.2(58)	34.1(34)	33.1(15)
OW(7)	x	0.194(2)	0.193(2)	0.196(2)	0.194(2)	0.218(3)	0.205(1)
96 (g)	y	0.229(2)	0.233(2)	0.235(2)	0.278(3)	0.240(4)	0.233(1)
	z	0.421(1)	0.421(2)	0.419(1)	0.415(3)	0.414(3)	0.416(1)
	occupancy	55.9(24)	62.1(25)	63.1(20)	93.1(77)	37.4(48)	54.3(16)
OW(8)	x	0.213(2)	0.221(3)	0.219(2)	0.202(7)	0.224(3)	0.213(2)
96 (g)	y	0.367(3)	0.381(3)	0.380(3)	0.372(11)	0.386(4)	0.393(2)
	z	0.296(3)	0.280(3)	0.278(2)	0.294(7)	0.272(4)	0.287(3)
	occupancy	35.7(23)	43.2(39)	46.3(26)	26.9(68)	35.5(48)	30.5(20)
OW(9)	x	0.327(1)	0.329(2)	0.329(2)	0.302(5)	0.364(4)	0.354(2)
96 (g)	y	0.391(1)	0.394(2)	0.398(2)	0.402(2)	0.403(4)	0.415(2)
	z	0.294(1)	0.296(2)	0.296(2)	0.304(5)	0.301(3)	0.302(2)
	occupancy	46.8(12)	39.5(18)	39.6(22)	77.8(39)	24.9(25)	26.8(12)

Table 1 (Continued)

		Na-LSX	NaK-LSX20	NaK-LSX42	NaK-LSX80(Na)	NaK-LSX80(K)	K-LSX
OW(10)	*x*	0.302(1)	0.304(2)	0.308(1)	0.320(3)	0.300(2)	0.309(2)
96 (g)	*y*	0.415(2)	0.413(2)	0.415(2)	0.451(4)	0.430(2)	0.423(2)
	z	0.182(2)	0.187(2)	0.188(2)	0.201(3)	0.186(2)	0.183(1)
	occupancy	57.0(25)	60.6(30)	65.9(24)	49.9(87)	73.7(33)	48.4(22)

[a] $R = (\sum|F_o^2 - SF_c^2|)/\sum|F_o^2|$. [b] $\chi^2 = (\sum w(F_o^2 - SF_c^2)^2)/(N_{obs} - N_{var})$. Definitions given by VonDreele.[15] [c] U_{iso} for Si and Al constrained to have same values for each model. [d,f] U_{iso} for framework oxygens and water molecules, respectively constrained to have same values for each model. [e,g–l] U_{iso} constrained to have same values, respectively. Naming scheme for each atom follows that given by Olson.[18] The estimated standard deviations are in parentheses.

study follows Olson's nomenclature (Figure 1 and Tables 1-3).[18]

The distribution of extraframework cations and water molecules could be determined at sites I, I′, and II on the basis of the principles outlined by Olson.[18–20] It was found to be consistent with the refinement results described below (Table 1). The Na^+ ions and water molecules have about the same atomic scattering factors, however. This, coupled with the possible disordering at weakly bound sites, makes unambiguous assignment of the species occupying sites III and III′ difficult.[21] The scattering factor for O^{2-} was used to model these supercage species. Some positions near site III showed close interatomic distances to framework oxygens, O(1) and O(4), and to the surrounding water molecules, suggesting these are possible locations of the disordered cation–water mixtures.

Isotropic displacement factors were included at the final stage of each refinement. Constraints were applied as stated in Table 1 with certain sets of atoms. The final residuals for each refinement as well as the final refined models are given in Table 1. Framework interatomic distances and angles are listed in Table 2, and Tables 3 summarizes interatomic distances involving extraframework cations. Possible interaction distances involving water molecules can be provided by authors upon request.

In the **Na-LSX** sample (Figures 2 and 3), only sodium ions were expected to be distributed over sites I, I′, II, and III′ as charge compensating cations, based on the ICP elemental analysis result. Rietveld analysis (Figure 3) revealed that sodium ions are coordinated by six O(3) oxygens at site I, by three O(3) oxygens at site I′ and by three O(2) oxygens at site II with the following interatomic distances: Na1–O(3) = 2.629(4) Å, Na2–O(3) = 2.375(5) Å and Na3B–O(2) = 2.348(5) Å (Table 3). The Na^+ ions at sites I′ and II are also coordinated to the nearby water molecules in the sodalite cage and in the supercage with the following interatomic distances: Na2–OW(2) = 2.497(8) Å and Na3B–OW(4) = 2.293(23) Å (Table 3).

Compared with Olson's model of hydrated $Na_{88}X$,[18] which was used as the initial model for this refinement, small but important differences in cation distributions are found in Na-LSX with Si/Al = 1.0. Hydrated $Na_{88}X$ has 12 Al_6 prisms and 4 Al_4 prisms in the unit cell. Only Al_6 prisms can have charge compensating cations at site I or I′, as mentioned before.[18–20] Accordingly, Olson's model shows that 8 Al_6 prisms have Na^+ ions at site I, and 4 Al_6 prisms have Na^+ ions at site I′, satisfying $8(I) \leq {}^1/_2[32 - 8(I')]$ for faujasites with Si/Al ≥ 1.[22] In the LSX framework, however, all the 16 hexagonal prisms per unit cell are Al_6 prisms. Consequently, the Na-LSX model from this study shows that 11 Al_6 prisms have Na^+ ions at site I, and the remaining 5 Al_6 prisms have Na^+ ions at site I′, satisfying $11(I) = {}^1/_2[32 - 10(I')]$ for LSX with Si/Al = 1.0. A similar situation arises at site II above the 6-ring windows in the supercage (Figure 1). Having 24 Al_3 6-rings, hydrated $Na_{88}X$ shows exactly 24 Na^+ ions at site II, whereas nearly full occupancy of Na^+ ions at site II (29.6(6) among 32 Al_3 6-rings) is observed in the Na-LSX unit cell.

Among the seven sites in the supercage refined as water molecules, OW(7) and OW(10) are close to framework oxygens, O(1) and O(4). The interaction distances are OW(7)–O(1) = 2.754(26) Å, OW(7)–O(4) = 2.879-(24) Å, OW(10)–O(1) = 2.691(28) Å, and OW(10)–O(4) = 2.838(28). These sites are also close to the surrounding water molecules, OW(5), OW(6), and OW(8). It was thus concluded these are the site III′ positions occupied by the disordered mixtures of Na^+ ions and water molecules.

The OW(1) water molecule at site I′ can hydrogen bond to three O(3) framework oxygens with an interatomic distance of 2.63(1) Å and to the OW(2) water molecule at site II′ in the sodalite cage with an interatomic distance of 2.62(1) Å. The OW(2) water molecule can also coordinate to the Na^+ ions at sites I′ with an interatomic distance of 2.50(1) Å and hydrogen bond to each other in the range of 2.56–2.86 Å. The OW(4) water molecule in the supercage coordinates to the Na^+ ions at site II with an interatomic distance of 2.29(3) Å (Table 3) and to the other water molecules in the supercage within the range of 2.53–3.16 Å.

On the basis of its unit cell formula (Table 1), the **NaK-LSX20** (Figures 2 and 4) sample was expected to have 19 K^+ ions and 77 Na^+ ions distributed over the available extraframework sites. At this level of ion exchange, the Na^+ ions at sites I′ and II were partially replaced by K^+ ions, as determined from Rietveld analysis (Figure 4). This distinction was made from the successive Fourier difference maps by considering both the mean Na^+–O and K^+–O distances and the possible cationic occupancies at sites I, I′ (Al_6 prisms), and II (Al_3 6-rings), as discussed before.[18–20] In the refined model, sodium ions are coordinated by six O(3) oxygens at site I, three O(3) oxygens at site I′, and three O(2) oxygens at site II with the following interatomic distances: Na1–O(3) = 2.584(4), Na2–O(3) = 2.365(6) Å, and Na3B–O(2) = 2.347(6) Å. Potassium ions are coordinated by three O(3) and O(2) oxygens at sites I′ and II with the following interatomic distances, respectively: K2–O(3) = 2.684(6) Å and K3B–O(2) = 2.770(9) Å (Table 3).

(21) Baur, W. H. *Am. Mineral.* **1964**, *49*, 697.
(22) Mortier, W. J.; Bosmans, H. J.; Uytterhoeven, J. B. *J. Phys. Chem.* **1972**, *76*, 650.

Table 2. Framework Interatomic Distances (Å) and Angles (degrees)

	Na-LSX[a]		NaK-LSX20[a]		NaK-LSX42[a]		NaK-LSX80(Na)[a]		NaK-LSX80(K)[a]		K-LSX[a]	
	T(1):Si	T(2):Al	T(1):Si	T(2):Al	T(1):Si	T(2):Al	T(1):Si	T(2):Al	T(1):Si	T(2):Al	T(1):Si	T(2):Al
T−O(1)	1.620(4)	1.729(2)	1.622(4)	1.731(2)	1.621(4)	1.731(1)	1.619(6)	1.728(2)	1.620(6)	1.729(2)	1.625(4)	1.736(2)
T−O(2)	1.622(4)	1.730(2)	1.623(4)	1.729(2)	1.620(4)	1.728(2)	1.620(7)	1.729(2)	1.621(6)	1.729(2)	1.618(4)	1.730(2)
T−O(3)	1.621(2)	1.731(2)	1.621(2)	1.730(2)	1.620(2)	1.729(2)	1.620(2)	1.729(2)	1.620(2)	1.729(2)	1.623(2)	1.731(2)
T−O(4)	1.619(2)	1.729(2)	1.622(2)	1.730(2)	1.620(2)	1.728(2)	1.621(2)	1.730(2)	1.621(2)	1.730(2)	1.621(2)	1.730(2)
mean	1.621(2)[b]	1.730(1)[b]	1.622(2)[b]	1.730(1)[b]	1.620(2)[b]	1.729(1)[b]	1.620(3)[b]	1.729(1)[b]	1.621(3)[b]	1.729(1)[b]	1.622(2)[b]	1.732(1)[b]
O(1)−O(2)	2.684(6)	2.862(6)	2.706(7)	2.856(6)	2.699(7)	2.861(6)	2.673(9)	2.810(7)	2.664(8)	2.806(7)	2.703(7)	2.818(6)
O(1)−O(3)	2.653(6)	2.792(5)	2.635(6)	2.788(5)	2.645(6)	2.785(5)	2.686(9)	2.760(7)	2.688(8)	2.771(6)	2.683(6)	2.815(5)
O(1)−O(4)	2.569(5)	2.806(4)	2.577(5)	2.798(4)	2.590(5)	2.782(4)	2.538(8)	2.848(6)	2.547(6)	2.846(5)	2.592(5)	2.831(5)
O(2)−O(3)	2.636(6)	2.814(4)	2.629(6)	2.825(4)	2.611(6)	2.827(4)	2.679(9)	2.798(5)	2.676(8)	2.797(5)	2.626(6)	2.808(5)
O(2)−O(4)	2.665(5)	2.791(5)	2.671(5)	2.792(5)	2.667(5)	2.799(5)	2.614(12)	2.854(6)	2.612(9)	2.855(6)	2.608(6)	2.786(5)
O(3)−O(4)	2.667(5)	2.879(4)	2.667(5)	2.889(4)	2.658(5)	2.881(5)	2.669(6)	2.867(5)	2.676(6)	2.863(6)	2.670(5)	2.903(5)
mean	2.646(3)[b]	2.824(2)[b]	2.648(3)[b]	2.825(2)[b]	2.645(3)[b]	2.823(2)[b]	2.643(4)[b]	2.823(3)[b]	2.644(4)[b]	2.823(3)[b]	2.647(3)[b]	2.827(3)[b]
T(1)−T(2)	3.119(3)		3.110(3)		3.113(3)		3.187(4)		3.202(4)		3.186(4)	
T(1)−T(2)	3.156(3)		3.150(3)		3.150(3)		3.191(6)		3.227(5)		3.225(4)	
T(1)−T(2)	3.085(3)		3.069(3)		3.077(3)		3.225(4)		3.157(4)		3.083(3)	
T(1)−T(2)	3.195(3)		3.211(3)		3.201(3)		3.033(5)		3.119(5)		3.199(4)	
mean	3.139(2)[b]		3.135(2)[b]		3.135(2)[b]		3.159(3)[b]		3.176(3)[b]		3.173(2)[b]	
O(1)−T−O(2)	111.8(3)	111.7(4)	113.0(3)	111.3(4)	112.9(3)	111.7(4)	111.2(4)	108.7(4)	110.6(4)	108.5(4)	113.0(4)	108.8(4)
O(1)−T−O(3)	109.9(4)	107.6(3)	108.7(4)	107.3(3)	109.4(4)	107.2(3)	112.1(5)	105.9(4)	112.1(4)	106.5(4)	111.4(4)	108.6(4)
O(1)−T−O(4)	104.9(4)	108.5(3)	105.2(4)	107.9(3)	106.1(4)	107.1(3)	103.2(7)	110.9(4)	103.6(6)	110.8(4)	106.0(4)	109.6(3)
O(2)−T−O(3)	108.8(4)	108.8(3)	108.3(4)	109.5(3)	107.4(4)	109.8(3)	111.5(7)	108.0(3)	111.4(6)	107.9(3)	108.3(4)	108.4(3)
O(2)−T−O(4)	110.6(3)	107.6(3)	110.8(3)	107.7(3)	110.8(3)	108.2(3)	107.5(6)	111.2(4)	107.4(5)	111.2(4)	107.3(4)	107.3(3)
O(3)−T−O(4)	110.8(3)	112.6(3)	110.7(3)	113.2(3)	110.3(3)	112.9(3)	110.9(4)	112.0(4)	111.3(4)	111.7(4)	110.8(3)	114.0(3)
mean	109.5(2)[b]	109.5(2)[b]	109.5(2)[b]	109.5(2)[b]	109.5(2)[b]	109.5(2)[b]	109.4(3)[b]	109.5(2)[b]	109.4(3)[b]	109.4(2)[b]	109.5(2)[b]	109.5(2)[b]
T(1)−O(1)−T(2)	134.2(3)		132.5(3)		133.3(3)		148.9(8)		141.0(6)		133.1(4)	
T(1)−O(2)−T(2)	140.6(3)		140.1(3)		140.4(3)		144.6(5)		148.9(5)		148.8(4)	
T(1)−O(3)−T(2)	137.1(3)		136.3(3)		136.8(3)		144.2(4)		145.9(4)		143.5(4)	
T(1)−O(4)−T(2)	145.2(3)		146.6(3)		145.9(4)		129.7(4)		137.1(4)		145.5(4)	
mean	139.3(2)[b]		138.9(2)[b]		139.1(2)[b]		141.9(3)[b]		143.2(3)[b]		142.7(2)[b]	

[a] Estimated standard deviations are in parentheses. [b] Standard deviation computed using $\sigma = 1/n[\sum\sigma^2]^{1/2}$.

Table 3. Interatomic Distances (Å) Involving Extra Framework Cations

	Na-LSX[a]	NaK-LSX20[a]	NaK-LSX42[a]	NaK-LSX80(Na)[a]	NaK-LSX80(K)[a]	K-LSX[a]
Na1−O(2)	3.634(4)	3.630(4)	3.625(4)	3.647(6)		
Na1−O(3)	2.629(4)	2.584(4)	2.605(4)	2.950(9)		
Na1−Na2[b]	2.66(1)	2.61(2)	2.65(2)	2.37(2)		
Na1−K2		3.19(1)	3.20(1)	3.33(2)		
K1−O(2)				3.647(6)	3.589(6)	3.559(4)
K1−O(3)				2.950(9)	2.898(9)	2.782(5)
K1−Na2[b]				2.37(2)		
K1−K2[b]				3.33(2)	3.18(2)	
Na2−O(2)	3.096(4)	3.081(5)	3.081(5)	3.034(7)		
Na2−O(3)	2.375(5)	2.365(6)	2.379(6)	2.361(6)		
Na2−K2[b]		0.58(2)	0.55(2)	0.96(3)		
Na2−OW(2)	2.50(1)	2.52(2)	2.53(2)	2.51(2)		
K2−O(2)		3.245(5)	3.239(5)	3.276(9)	3.240(8)	
K2−O(3)		2.684(6)	2.680(6)	2.737(7)	2.735(7)	
K2−OW(2)		2.75(2)	2.74(2)	2.80(2)	2.79(2)	
Na3B−O(2)	2.348(5)	2.347(6)	2.347(8)	2.201(17)	2.370(31)	
Na3B−O(4)	3.077(5)	3.091(5)	3.089(6)	2.997(13)	2.961(10)	
Na3B−K3B[b]		0.88(2)	0.90(2)	1.31(9)	0.97(11)	
Na3B−OW(2)		3.15(2)	3.06(3)	3.08(10)	2.74(12)	
Na3B−OW(4)	2.29(3)	2.30(5)	2.42(7)			
K3B−O(2)		2.770(9)	2.788(6)	2.732(13)	2.777(10)	2.792(5)
K3B−O(4)		3.362(8)	3.368(6)	3.183(13)	3.147(10)	3.115(5)
K3B−OW(4)				2.75(6)	3.15(4)	3.45(4)
K3B−OW(4B)		2.79(2)	2.78(2)	2.62(7)	2.57(3)	2.73(2)
K3B−OW(5)		3.32(2)	3.32(2)			3.01(4)
K3B−OW(6)				2.89(9)		
K3B−OW(8)		3.30(7)	3.27(5)	3.37(25)	3.49(9)	

[a] The value in parentheses is the estimated standard deviation. [b] Simultaneous occupancy by these atoms is excluded.

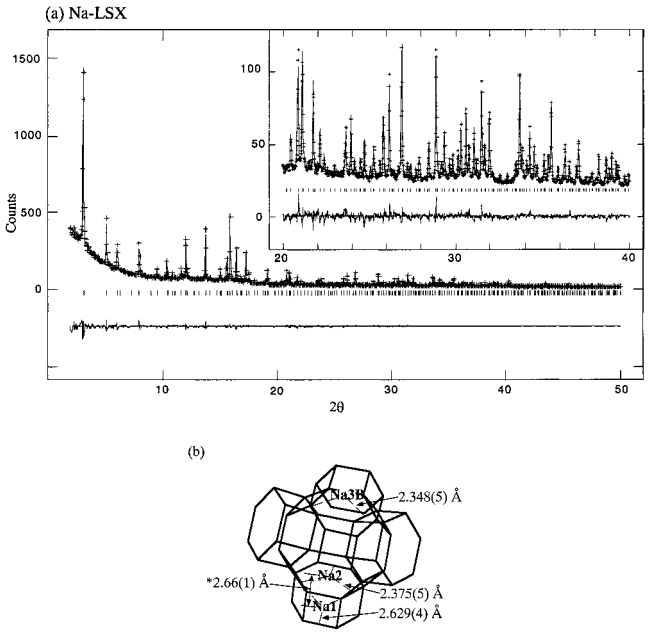

Figure 3. (a) Calculated (continuous line) and observed (crosses) synchrotron X-ray powder diffraction profiles for the Na-LSX sample at room temperature. A difference curve ($I_{obs} - I_{calc}$) is plotted at the bottom on the same scale. Allowed reflection positions are indicated by vertical lines. (b) Schematic diagram describing cation distribution of the Na-LSX model from the refinement. One sodalite cage and four double 6-rings are shown (see Tables 1 and 3). *Simultaneous occupancy does not occur.

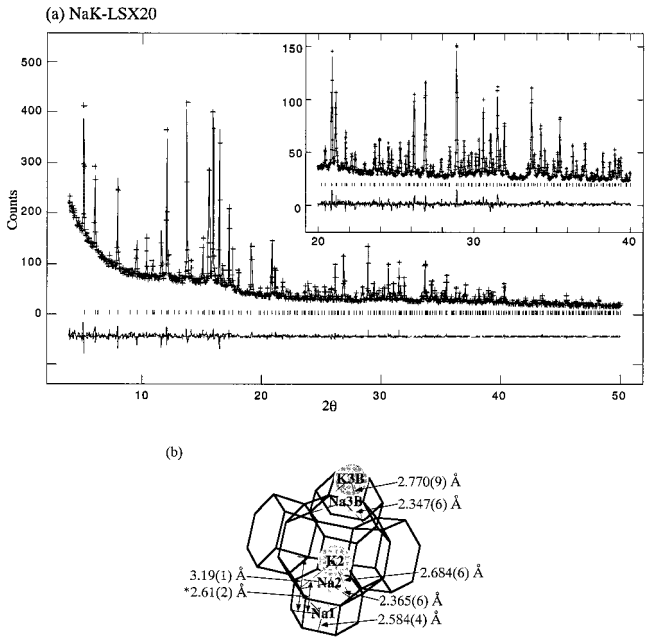

Figure 4. (a) Calculated (continuous line) and observed (crosses) synchrotron X-ray powder diffraction profiles for the NaK-LSX20 sample at room temperature. A difference curve ($I_{obs} - I_{calc}$) is plotted at the bottom on the same scale. Allowed reflection positions are indicated by vertical lines. The first (111) peak is not included in this figure. (b) Schematic diagram describing cation distribution of the NaK-LSX20 model from the refinement (see Tables 1 and 3). *Simultaneous occupancy does not occur.

Close examination of the changes in the site occupancies between the Na-LSX and NaK-LSX20 models (Table 1) suggests that as K^+ ions replace the Na^+ ions at site I′, some of these Na^+ ions migrate into site I, at the center of the double 6-ring. The number of Na^+ ions at site I′ decreased from 9.3(5) to 2.2(5), while that of the Na^+ ions at site I increased from 11.3(3) to 14.9(3) as 8.2(4) K^+ ions occupied site I′ in the NaK-LSX20 sample (Table 1). In this sample, simultaneous occupancy by the Na^+ ions at site I and the K^+ ions at site I′ was made possible while that of the Na^+ ions at sites I and I′ was avoided by the close intercationic distance: Na1−K2 = 3.19(1) Å and Na1−Na2 = 2.61(2) Å (Table 3).

The number of Na^+ ions at site II also decreased from 29.6(5) to 21.9(8) as 9.0(5) K^+ ions occupied this site.

The total number of K^+ ions located at sites I′ and II is 17.2(9) per unit cell, which is close to 19, as determined from the ICP elemental analysis result. Sites I′ and II are preferred by K^+ ion at the early stage of K^+ exchange.

The distribution of the site III′ species in NaK-LSX20 is similar to that in Na-LSX. The OW(7) and OW(10) water molecules show close interatomic distances to framework oxygens with OW(7)−O(1) = 2.68(3) Å, OW(7)−O(4) = 2.92(3) Å, OW(10)−O(1) = 2.76(4) Å, and OW(10)−O(4) = 2.98(4) Å. The distribution of the other supercage species is also comparable to that found in Na-LSX, except for the presence of the OW(4B) water molecule above site II in the case of NaK-LSX20. This site for water molecules becomes populated as K^+ ions enter site II. The OW(4B)−K3B distance is 2.79(2) Å. In the sodalite cage, the increased number of OW(2) water molecules from 25.9(7) to 35.1(8) reflects the transfer of the OW(1) water molecule at site I′ to the OW(2) position as K^+ ions occupy site I′. Other possible interaction distances involving water molecules and K^+ ions are as follows: OW(2)−K2 = 2.75(2) Å, OW(5)−K3B = 3.32(2) Å, and OW(8)−K3B = 3.30(7) Å (Table 3).

The **NaK-LSX42** sample (Figure 2), which was equilibrated at 42% of K^+-exchange level, shows a similar cation distribution to that found in NaK-LSX20. The coordination distances between extraframework cations and framework oxygens are Na2−O(3) = 2.379(6) Å, K2−O(3) = 2.680(6) Å, Na3B−O(2) = 2.347(8) Å, and K3B−O(2) = 2.788(6) Å (Table 3). At this level of ion exchange, however, there were increased numbers of K^+ ions at both sites I′ and II with 9.4(4) and 17.3(5), respectively (Table 1). The number of Na^+ ions at site I′ has decreased further to 1.4(4), following the ion exchange behavior at sites I and I′, as observed from the previous refinements. Repositioning the Na^+ ions at site I′ into site I as more K^+ ions occupied site I′ was almost completed at this stage, achieving nearly full occupancy of site I by Na^+ ions (Table 1).

Among the total of 40 K^+ ions per unit cell in this sample, only 26.7(9) were located at sites I′ and II, implying that the remaining K^+ ions were disordered at site III′. Accordingly, the OW(8) position shows close interatomic distances to framework oxygens along with OW(7) and OW(10), suggesting that this is a new site III′ occupied by the disordered mixtures of cations and water molecules. The number of OW(4B) water molecules increased from 9.6(13) to 15.7(13) as that of the coordinating K3B ions increased from 9.0(6) to 17.3(5), suggesting a correlation between these two species. Possible water to cation interaction distances are as follows: OW(2)−Na2 = 2.53(2) Å, OW(2)−K2 = 2.74(2) Å, OW(4)−Na3B = 2.42(7) Å, and OW(4B)−K3B = 2.78(2) Å (Table 3).

The **NaK-LSX80** sample shows peaks attributed to two distinct face-centered cubic unit cells (Figures 2 and 5). Each peak from the original phase has a corresponding peak at lower 2θ indicating a larger but related unit cell for the new phase. To our knowledge, this is the first observation of a phase transition during exchange of alkali metal into X or Y type zeolites. Similar observations were reported using Sr^{2+}−Na^+ exchange into Linde X type zeolite[23] and Ca^{2+}−Na^+ exchange into LSX type zeolite.[24] Rietveld refinement for the NaK-LSX80 sample revealed characteristic cation distribution for each phase (Figure 5), which is responsible for the phase transition. The phase with expanded lattice parameter (25.2086(5) Å), designated NaK-LSX80(K), is distinguished from the original phase by having K^+ ions at site I. The original phase, designated NaK-LSX80(Na), possesses a lattice parameter (25.0389(5) Å) similar to those of the Na-LSX, NaK-LSX20, and NaK-LSX42 samples (Table 1). This phase shows a mixed occupancy by Na^+ and K^+ ions at site I with the Na^+ ions as the major counterions (Table 1).

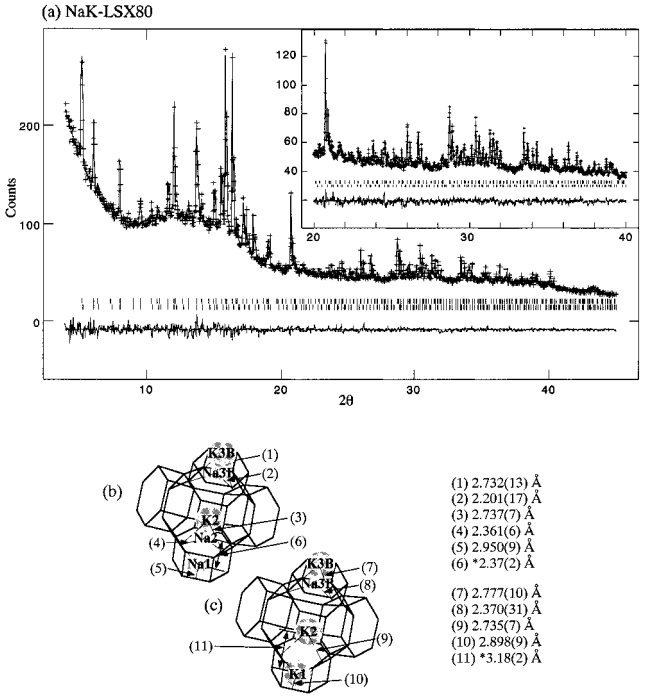

Figure 5. (a) Calculated (continuous line) and observed (crosses) synchrotron X-ray powder diffraction profiles for the NaK-LSX80 sample at room temperature. A difference curve ($I_{obs} - I_{calc}$) is plotted at the bottom on the same scale. Allowed reflection positions are indicated by vertical lines for each phase. The first (111) peak of each phase is not included in this figure. Schematic diagrams describing cation distribution of (b) the NaK-LSX80(Na) phase and (c) the Na-LSX80(K) phase from the refinement (see Tables 1 and 3). *Simultaneous occupancy does not occur.

The diffusion mechanism of K^+ ions into site I, which resulted in the lattice parameter expansion, can be monitored by inspecting the changes in the T−O−T angles which are associated with the double 6-ring. These angles are the T−O(1)−T, T−O(2)−T and T−O(3)−T, shown in Figure 6. The angles remain unchanged within experimental error up to 42% K^+-exchange level. For the NaK-LSX80(Na) phase, an increased number of K^+ ions around the 6-ring sites causes these angles to increase, facilitating the diffusion of K^+ ions into site I. Indeed, site I in the NaK-LSX80(Na) phase shows mixed occupancy by 10.9(6) Na^+ ions and 2.3(1) K^+ ions. This represents the maximum K^+ content for site I in the lower volume phase. Addition of more K^+ ions to

(23) Olson, D. H.; Sherry, H. S. *J. Phys. Chem.* **1968**, *72*, 4095.
(24) Kuhl, G. H.; Sherry, H. S., 5th International Zeolite Conference, Naples, 1980, 813.

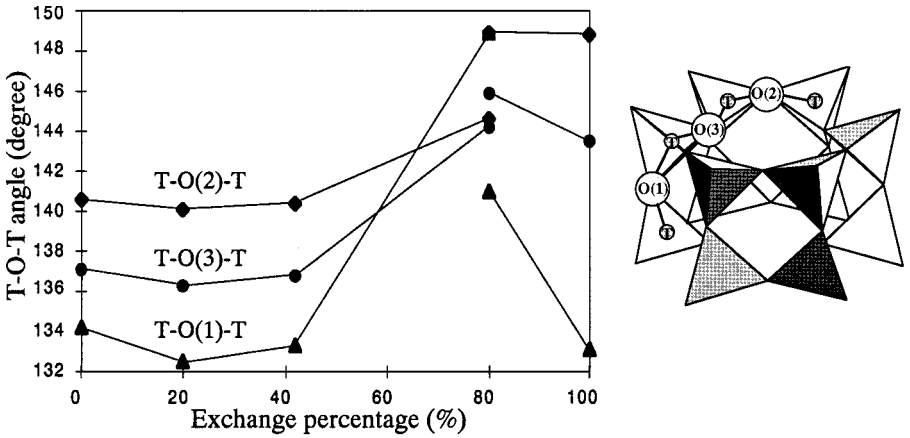

Figure 6. Variation of K^+-exchange percentage versus ⟨T−O−T⟩ angles. At 80% K^+ exchange, two phases are shown with each set of T−O−T angles. A schematic diagram illustrating some of the T−O−T angles associated with the double 6-ring is also shown (see Table 2).

this site results in the larger volume phase. Meanwhile, site I′ exhibits an increased Na^+ occupancy of 6(1), compared with the previous NaK-LSX42 model, presumably due to the reoccupation of the Na^+ ions from site I.

For the NaK-LSX80(K) phase, further increased T−O−T angles allow full replacement of the Na^+ ions at site I by K^+ ions. In this phase, Na^+ ions are all replaced from the small cavity system (sites I and I′), and only 5(1) Na^+ ions are found at site II in the supercage. The numbers of K^+ ions at sites I and I′ in the NaK-LSX80(K) phase (11.4(3) and 9.2(5), respectively), are comparable to those of Na^+ ions at sites I and I′ in the Na-LSX sample (11.3(3) and 9.3(5), respectively). Linear constraints[15] were used to avoid simultaneous occupancy by K^+ ions at these neighboring positions. The refined fraction of each phase was 0.37 and 0.63 for the NaK-LSX80(Na) and NaK-LSX80(K) phase, respectively.

The site III′ positions in both phases are similar along with the distribution of the other supercage species. The interatomic distances between the site III′ species, OW(7), OW(8), and OW(10), and framework oxygens, O(1) and O(4), are in the range of 2.78−3.37 Å, although a small amount of uncertainty arises from the different occupancies of these sites in each phase. The OW(4) water molecule which interacted with Na3B in the Na-LSX, NaK-LSX20, and NaK-LSX42 models has migrated to coordinate K3B as the number of Na3Bs decreases in both phases of the NaK-LSX80 sample. The OW(4B) water molecule continues to interact with K3B, with a further increased number in each phase as the number of K3Bs increases (Table 1). The corresponding interatomic distances are OW(4)−K3B = 2.75(6) Å and OW(4B)−K3B = 2.62(7) in the NaK-LSX80(Na) phase and OW(4)−K3B = 3.15(4) Å and OW(4B)−K3B = 2.57(3) in the NaK-LSX80(K) phase. Other possible interaction distances involving Na^+−water and K^+−water are in the range of 2.51−3.08 and 2.57−3.49 Å in both phases, respectively (Table 3).

The powder diffraction pattern of **K-LSX** (Figures 2 and 7) indicates the presence of one phase with a lattice parameter of 25.2486(2) Å in the sample. The distribution of K^+ ions determined from Rietveld refinement shows nearly full occupancies of sites I and II by 15.5(2) and 31.0(2) K^+ ions, respectively. The coordination

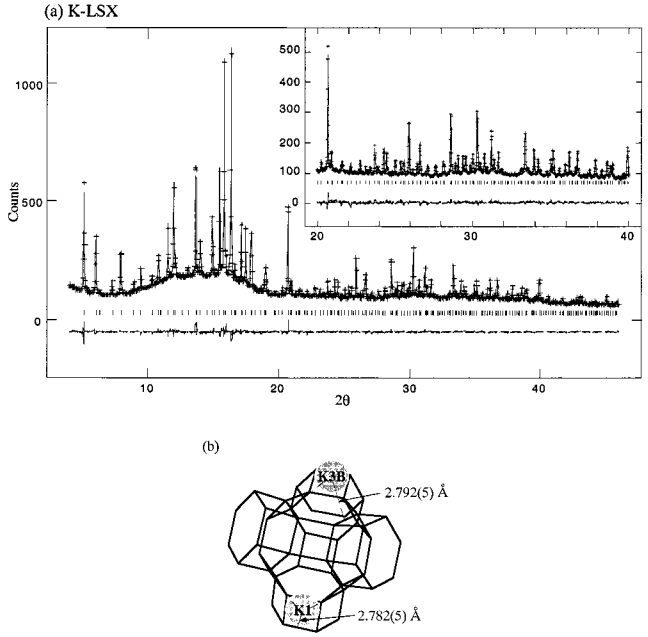

Figure 7. (a) Calculated (continuous line) and observed (crosses) synchrotron X-ray powder diffraction profiles for the K-LSX sample at room temperature. A difference curve ($I_{obs} - I_{calc}$) is plotted at the bottom on the same scale. Allowed reflection positions are indicated by vertical lines. The first (111) peak is not included in this figure. (b) Schematic diagram describing cation distribution of the K-LSX model from the refinement (see Tables 1 and 3)

distances are K1−O(3) = 2.782(5) Å and K3B−O(2) = 2.792(5) Å. Only water molecules are attributed to the electron density near site I′, since simultaneous occupancy by K^+ ions at these closely separated sites is unlikely; the separation between site I and site I′ is 3.27(2) Å. The full occupancy of site I by K^+ ions was not observed in the previous studies of hydrated $K_{86.5}X$.[22,25] No obvious explanation of the difference in behavior between the two samples of X is available at this stage. However, the fact that potassium is a necessary component in the gel from which LSX is formed may be related to this phenomenon. This is also analogous with a strong potassium-templating effect of the 18-crown-6 ether with a six oxygen donor set similar to the double 6-ring of LSX (Figure 6).

(25) Mortier, W. J.; Bosmans, H. J. *J. Phys. Chem.* **1971**, *75*, 3327.

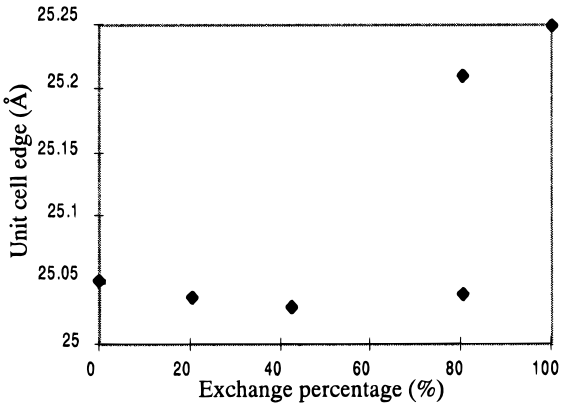

Figure 8. Variation of K^+-exchange percentage versus cell edge (a). At 80% K^+ exchange, two phases are shown with each cell edge value (see Table 1).

Upon acquiring full occupancy of site I by K^+ ions, the T−O−T angles show small decreases at the double 6-ring openings (Table 2 and Figure 6). The T−O(1)−T angle has also decreased as the large potassium ions fully occupy the double 6-ring site. The site III′ positions, occupied by OW(7), OW(8), and OW(10), exhibit close interatomic distances to framework oxygens, O(1) and O(4) in the range of 2.85−3.45 Å. The interaction distances between K3B and the supercage waters are in the range of 2.73−3.45 Å (Table 3), and the supercage waters can hydrogen bond to each other within 2.51−3.50 Å.

This work clearly illustrates how cation location can influence zeolite structures to a significant degree (Figure 8). The key here is the location of potassium at site I, the center of the double 6-ring. Careful examination of the X zeolite structure indicates that expansion or contraction of the double 6-ring potentially has the most impact on the structural parameters. The results from the current study have also revealed the presence of the site preferences of exchanging cations and its impact on structural responses on the atomistic scale. A more detailed exchange mechanism can be derived from the time-resolved studies.[7] For example, the on-going time-resolved investigations will be based on the results of the ex situ experiments described above and provide the complete pathway of the ion exchange reaction, which might be different from the present study performed on several equilibrated samples. Finally, these studies may form a basis by which properties such as the selective adsorption[26] behavior can be tailored as a function of different cation distributions and the structural phase transitions they induce.

Conclusions

At low levels of K^+ exchange into Na-LSX, potassium ions show preferences for replacing the Na^+ ions at site I′, located on both sides of the double 6-rings in the sodalite cages, and at site II, located above the single 6-rings in the supercages. The replacement at site I′ is accompanied by the repositioning of the Na^+ ions at site I′ into site I (Figure 1). At the 80% K^+-exchange level, two phases occur in the sample. The phase with the expanded cell volume has K^+ ions at site I, while the phase with the lower cell volume has Na^+ ions at site I. The mechanism of K^+ ion diffusion into site I can be monitored by examining the changes in the T−O−T angles, which define the double 6-ring entrances (T−O(2)−T and T−O(3)−T) as seen in Figure 6. At the 80% level of K^+ exchange, the T−O(2)−T and T−O(3)−T angles increase as K^+ ions replace the Na^+ ions at site I′, facilitating the diffusion of K^+ ions into site I. Full exchange of the Na^+ ions at site I by K^+ ions takes place in the expanded cell with more enlarged T−O−T angles. Sites I and II are fully occupied by K^+ ions in the K^+ ion end member of LSX.

Acknowledgment. The authors thank David E. Cox, J.-H. Park, and Christopher L. Cahill for their help with data collection at X7A, which is supported by a grant from the US-DOE Division of Chemistry and Materials Sciences, and we thank Florence Hollway and Jeremy Hopwood. Special thanks also to Prof. Scott McLennan for chemical analysis and Dr. Guenter H. Kuhl and Dr. Geoffrey M. Johnson for valuable suggestions. The work was supported by a grant from the NSF DMR-9713375.

Supporting Information Available: A table of possible interatomic distances involving water molecules (3 pages). Ordering information is given on any current masthead page.

CM980342S

(26) Coe, C. G.; Gaffney, T. R.; Kirner, J. F.; Klotz, H. C.; MacDougall, J. E.; Toby, B. H. 211th National Meeting of the American Chemical Society, New Orleans, LA, 1996, AN 1996:221366.